Available online at www.sciencedirect.com
ScienceDirect
Journal of Power Sources 159 (2006) 824–835
JOURNAL OF POWER SOURCES
www.elsevier.com/locate/jpowsour

Parameters estimation of a PEM fuel cell polarization curve and analysis of their behavior with temperature

M.G. Santarelli *, M.F. Torchio, P. Cochis

Dipartimento di Energetica, Politecnico di Torino, Corso Duca degli Abruzzi 24, 10129 Torino, Italy

Received 21 January 2005; received in revised form 3 August 2005; accepted 26 November 2005
Available online 18 January 2006

Abstract

The paper shows and discusses a procedure of parameter estimation applied to the evaluation of some operating parameters of a proton-exchange membrane fuel cell (PEMFC). First, a brief literature review about the main parameters (exchange current density, cell resistance, internal current density and limiting current density) has been done. Then the analytical model adopted to describe the polarization curve has been discussed. Based on this model, a parameter analysis has been done, and it has been shown that three parameters of the cell polarization curve model can be simultaneously estimated: the cathode exchange current density, the cell resistance and the internal current density. To evaluate these parameters both a set of our measurements on a PEM single cell (active area of 25 cm^2 and Nafion 115 membrane) and data from other authors has been considered.

The cell has been fed with pure hydrogen and air, the cell temperature has been varied from 50 °C to 80 °C, and accordingly the reactants have been introduced in the cell humidified at the same temperature. The parameters have been estimated in each operating conditions of the cell, and their behavior, as a function of the cell operating temperature, has been discussed.

Keywords: PEMFC; Cathode exchange current; Cell resistance; Internal current; Parameters estimation

1. Introduction and aims of the paper

The performance of a proton-exchange membrane fuel cell (PEMFC) can be expressed through the analytical formulation of the polarization curve [1,2]; different approaches could be considered, and the models formulation introduces some operating parameters. Among the most important parameters are: exchange current density at the anode $i_{0,a}$ and cathode $i_{0,c}$ electrodes; cell resistance r; internal current density i_n; limiting current density at the anode $i_{l,a}$ and cathode $i_{l,c}$ electrodes. In literature, the discussion about the simultaneous estimation of the previous parameters is not particularly developed. Besides that, there are few evaluations concerning the behavior of the cell parameters versus cell operating temperature. Therefore, this paper starts with an analysis about the available literature concerning the cell parameters evaluation. Then, a regression model of the polarization curve, adopted for the parameter estimation procedure, is described, and the characteristic parameters are outlined. After, the parameter estimation procedure (inverse model [3]) is described, which makes use of the experimental data of the independent variables (such as current density and operating temperature) and the dependent variables (such as cell voltage). Some preliminary tests made on the model showed the number and type of parameters which had been possible to correctly estimate from the experimental data. After, the main parameters of the polarization curve of a single PEM have been estimated (a brief description of the experimental setup and of the fuel cell adopted is also provided). Then, the behavior of the estimated parameters as a function of an independent variable (cell operating temperature) has been discussed. Finally, the parameter estimation procedure has been extended to other sets of experimental data and the agreements and discrepancies are discussed.

2. Brief literature analysis

A wide and detailed discussion about these parameters is available in literature.

* Corresponding author. Tel.: +39 011 564 4487; fax: +39 011 564 4499.
E-mail addresses: massimo.santarelli@polito.it (M.G. Santarelli), marco.torchio@polito.it (M.F. Torchio).

0378-7753/$ – see front matter © 2005 Elsevier B.V. All rights reserved.
doi:10.1016/j.jpowsour.2005.11.099

Nomenclature

a	activity of a substance
Bp	backpressure of reactants (bar)
c	concentration of a chemical species (mol m^{-3})
c_∞	concentration of a chemical species before the diffusion layer (mol m^{-3})
C_1	parameter of the cell resistance expression (Ω cm^2)
C_2	parameter of the cell resistance expression (Ω cm^4 A^{-1})
D	diffusivity of a chemical species (cm^2 s^{-1})
E	open circuit voltage of the single PEM fuel cell (V)
F	Faraday number (96,485 C mol^{-1})
$\bar{g}$	molar Gibbs free energy (J mol^{-1})
i	current density (A cm^{-2})
i_l	limiting current density in a PEM fuel cell (A cm^{-2})
$i_{l,a}$	anode limiting current density (A cm^{-2})
$i_{l,c}$	cathode limiting current density (A cm^{-2})
i_n	internal current density
$i_{0,a}$	anode exchange current density (A cm^{-2})
$i_{0,c}$	cathode exchange current density (A cm^{-2})
$i_{0,el}$	exchange current density in an electrode (A cm^{-2})
I	current (A)
$\bar{M}$	molar mass (g mol^{-1})
n	number of electrons participating in a reaction
n_d	electro-osmotic drag coefficient (mol$_{H_2O}$ mol$^{-1}_{H^+}$)
N	molar flux per surface area (mol s^{-1} cm^{-2})
p	partial pressure of a gas (bar)
PEMFC	proton-exchange membrane fuel cell
r	cell resistance of the PEM fuel cell (Ω cm^2)
r^{el}	electronic resistance (Ω cm)
r^{ion}	ionic resistance (Ω cm^2)
R	universal gas constant (J mol^{-1} K^{-1})
t_m	membrane thickness (cm)
T	temperature (°C)
T_a^S	temperature of saturated inlet anode flow (°C)
T_c^S	temperature of saturated inlet cathode flow (°C)
V_c	voltage of the single PEM fuel cell (V)

Greek letters

α^a	anode transfer coefficient
α^c	cathode transfer coefficient
α_a^{el}	transfer coefficient on an electrode
α_c^{el}	transfer coefficient on an electrode
δ	Nernst diffusion layer thickness (cm)
ε_π	percolation threshold
γ	empirical constant of diffusivity correction
η	overpotential (V)
η_{act}	activation overpotential (V)
$\eta_{act,a}$	anode activation overpotential (V)
$\eta_{act,c}$	cathode activation overpotential (V)
η_{conc}	concentration overpotential (V)
$\eta_{conc,a}$	anode concentration overpotential (V)
$\eta_{conc,c}$	cathode concentration overpotential (V)
η_{ohm}	ohmic overpotential (V)
λ	degree of humidification of the membrane (mol$_{H_2O}$ mol$^{-1}_{SO_3^-}$)
λ_{H_2}	hydrogen excess
λ_{air}	air excess
σ	membrane ionic conductivity (Ω cm)$^{-1}$

2.1. Exchange current density

It pertains to the specific electrochemical reaction, and it is mainly a function of the electrode characteristics: type and quantity of catalyst, dimension and distribution of the catalyst particles, active surface. Considering the operation variables, it is linked especially to the cell temperature.

The catalyst type has an important role. Some indicatives values, related to the anode electrode of a PEM at $T = 25$ °C: Ag, $i_{0,a} = 4 \times 10^{-4}$ A cm^{-2}; Ni, $i_{0,a} = 6 \times 10^{-3}$ A cm^{-2}; Pt, $i_{0,a} = 5 \times 10^{-1}$ cm^{-2} [4].

The increase of the operation temperature would cause an increase of the exchange current density, because a higher temperature value allows an improvement of the reaction activation [4].

In a PEM fuel cell, the value of the exchange current density at the cathode electrode is considerably low compared to the value at the anode electrode, and therefore the anodic activation overvoltage are usually negligible. As an example, typical values are: $i_{0,a} = 0.2$ A cm^{-2} and $i_{0,c} = 1 \times 10^{-4}$ A cm^{-2} [4]. In ref. [5], a value of $i_0 = 1 \times 10^{-4}$ A cm^{-2} is considered, even if it is not explained whether at the anode or (probably) at the cathode side. In ref. [6], the values are: $i_{0,a} = 0.0538$ A cm^{-2} and $i_{0,c} = 1.0764 \times 10^{-6}$ A cm^{-2} at $T = 25$ °C; in the paper, an analytical expression of the exchange current density, taken from Berger [7] and associated to a generic electrode reaction $a\mathrm{A} + n\mathrm{e}^- \leftrightarrow b\mathrm{B}$, is also described:

$$i_0 = n \cdot F \cdot k^0 \cdot \left[\exp\left(\frac{-\Delta F_e}{R \cdot T} \right) \cdot c_A^{a \cdot (1-\alpha^{el})} \cdot c_B^{b \cdot \alpha^{el}} \right] \quad (1)$$

where ΔF_e is defined as free standard energy of activation, which is finally the change of the Gibbs free energy of reaction, while k^0 is a parameter connected to the reaction speed. In ref. [8], there are two different analytical expressions related to the anode and cathode exchange current density:

$$i_{0,a} = n_a \cdot F \cdot k_a \cdot \exp\left[\frac{(1-\beta) \cdot n_a \cdot F \cdot E^0}{R \cdot T} \right],$$

$$i_{0,c} = n_c \cdot F \cdot k_c \cdot \exp\left[\frac{-\beta \cdot n_c \cdot F \cdot E^0}{R \cdot T} \right] \quad (2)$$

In ref. [9], an exhaustive model of the polarization curve is described; in the model the anodic overvoltage is neglected, and the value of the cathode exchange current density is considered

$i_{0,c} = 0.01\ \mathrm{A\,cm^{-2}}$; it looks a high value, and it could be due to the fact that the cathode is fed with pure oxygen in place of air.

In refs. [10,11], a unique value is considered: $i_0 = 4.84 \times 10^{-8}\ \mathrm{A\,cm^{-2}}$; the low value could be explained with the materials of the electrodes, different from the usual carbon cloth; moreover, in the papers a dependence of the electrode activation from the ionic conductivity of the membrane electrolyte is described, thus introducing a further functional link. In ref. [12], the considered exchange current density value is: $i_0 = 1 \times 10^{-6}\ \mathrm{A\,cm^{-2}}$.

Finally, there is an interesting paper of Parthasarathy et al. [13], where the modification of the exchange current density value with the cell operation temperature is described. At low current density, the platinum particles in the catalyst layer are covered by oxidate particles (oxide-covered conditions) separating them from the oxygen reactant particles; therefore, at lower load the reaction speed decreases and thus the exchange current density: the values at the cathode electrode are in the range from $i_{0,c} = 6 \times 10^{-5}\ \mathrm{A\,cm^{-2}}$ at $T = 30\ ^\circ\mathrm{C}$ to $i_{0,c} = 2.6 \times 10^{-4}\ \mathrm{A\,cm^{-2}}$ at $T = 70\ ^\circ\mathrm{C}$.

2.2. Cell resistance

The ohmic overvoltage could be expressed by $\eta_{ohm} = r{\cdot}i = (r^{el} + r^{ion}){\cdot}i$, with the electronic ($r^{el}$) and ionic ($r^{ion}$) contributes. The electronic resistance increases with the operation temperature. The ionic resistance of the membrane is related to the operation temperature too, but especially to the degree of humidification of the membrane: in fact, the ionic conductivity of the Nafion increases with the membrane humidification. Therefore, the ionic conductivity could have a direct relationship with the current density (the load). In ref. [6], there is a analytic polynomial expression of the cell resistance found from experimental tests made with a single PEM cell of 50.56 $\mathrm{cm^2}$ active area and Nafion 117 membrane:

$$r = \gamma_1 + \gamma_2 \cdot T + \gamma_3 \cdot I \tag{3}$$

where $\gamma_1 = 0.811488\ \Omega\,\mathrm{cm^2}$, $\gamma_2 = -1.7696 \times 10^{-3}\ \Omega\,\mathrm{cm^2\,K^{-1}}$ and $\gamma_3 = 4.0488 \times 10^{-3}\ \Omega\,\mathrm{cm^2\,A^{-1}}$.

As we see, according to the empirical evaluation the cell resistance has to decrease with the operation temperature, and to increase with the current density. As an example, the value of the cell resistance r with $T = 343.15\ \mathrm{K}$ (70 °C) and $I = 10\ \mathrm{A}$ ($i = 0.2\ \mathrm{A\,cm^{-2}}$) is in the order of $r = 0.245\ \Omega\,\mathrm{cm^2}$.

In a further paper [14], Amphlett et al. introduce another analytical expression of the ionic resistance, deducted from the analysis of literature data related to different cells all with a Nafion 117 membrane:

$$r^{ion} = \frac{181.6 \cdot [1 + 0.03 \cdot i + 0.062 \cdot (T/303)^2 \cdot i^{2.5}]}{(\lambda - 0.634 - 3 \cdot i) \cdot \exp[4.18 \cdot ((T - 303)/T)]} \cdot t_m \tag{4}$$

The cell resistance is related to the membrane thickness t_m, to the operation temperature, to the current density and to the degree of humidification of the membrane λ. The parameter λ has been introduced by Springer et al. [9], and it is defined as the ratio between the number of water molecules and the number of sulfonic groups SO_3^- of the membrane.

Considering indicative values ($T = 70\ ^\circ\mathrm{C}$, $\lambda = 14$ corresponding to the situation of saturated reactant flows [15]) the ionic resistance increases with the load, with an approximate linear relationship with a slope $8.29 \times 10^{-4}\ \Omega\,\mathrm{m^2\,A^{-1}}$.

In ref. [9], an experimental procedure devoted to the determination of the degree of humidification of the membrane is described, which allows the evaluation of the ionic resistance in the case of Nafion 117: it decreases with the membrane humidification, and an indicative value with $T = 80\ ^\circ\mathrm{C}$ and $i = 0.5\ \mathrm{A\,cm^{-2}}$ is $r^{ion} = 0.285\ \Omega\,\mathrm{cm^2}$. The value described in Amphlett et al. [6] is lower because it is evaluated at lower current density ($0.2\ \mathrm{A\,cm^{-2}}$) and temperature (with a coherence with (3)).

In ref. [5], the cell resistance is evaluated at $T = 70\ ^\circ\mathrm{C}$ and $i = 1\ \mathrm{A\,cm^{-2}}$, with a value of $r = 0.15\ \Omega\,\mathrm{cm^2}$, without specifying the Nafion thickness (we suppose Nafion 115; otherwise, in case of Nafion 117, the value would not be coherent with the values reported by Amphlett and Springer, because it would mean a lower resistance in case of higher current density).

In ref. [16], considering a Nafion 115 membrane at different pressures and temperatures, in case of $p = 1$ atm at $T = 50\ ^\circ\mathrm{C}$ the resistance is evaluated as $r = 0.363\ \Omega\,\mathrm{cm^2}$, and at $T = 70\ ^\circ\mathrm{C}$ as $r = 0.238\ \Omega\,\mathrm{cm^2}$; so also in this analysis, the resistance r decreases with temperature. In ref. [17], Nafion 112, 115 and 117 membranes are analyzed in the range 70–80 °C, at different pressures, and the parameters of a polarization curve similar to the one proposed by Kim et al. [16], are estimated; in particular, in case of Nafion 115 operating at atmospheric pressure, at 70 °C the resistance is evaluated as $r = 0.24\ \Omega\,\mathrm{cm^2}$. Pisani et al. [18] derived a semi-empirical equation of the polarization curve take into account especially the cell voltage deterioration deriving from the cathode active region; they used the equation to fit the set of experimental data of [17]: concerning the cell resistance, in case of Nafion 115 fed by H_2/air, operating at atmospheric pressure, at 70 °C, $r = 0.24\ \Omega\,\mathrm{cm^2}$.

2.3. Internal current density

The internal current density is referred to the electrons transported through the electrolyte membrane and to the fuel crossover. This current is thus active even in open circuit conditions (equilibrium of the electrochemical reactions), and is related to the reduced value of the open circuit voltage (at the PEMFC temperature range, in the order of 0.9 V, see the graphs below) compared to the reversible voltage (in the order of 1.2 V). Its effect is introduced in term of an increase of the activation, ohmic and concentration overvoltages, and it is well known that the internal current i_n has to be reduced in order to increase the cell behavior. In the PEMFC literature, this parameter is usually neglected, or it is considered as a fixed value as $i_n = 2\ \mathrm{mA\,cm^{-2}}$ [4]. In ref. [19], in a paper describing the performances of a membrane operating at temperatures higher than 100 °C, an internal current density value of $i_n = 1\ \mathrm{mA\,cm^{-2}}$ is reported. The same author, in 2005 [20] analyzed another membrane (28 μm thick) and the internal current density is around $2\ \mathrm{mA\,cm^{-2}}$. In a recent paper [21], the authors underline the sensitivity of the model of

the polarization curve to the internal current density, which only affects the simulation results at low current values.

A paper where it seems to be introduced a concept related to the internal current density has been written by Kim et al. [16]. An analytical expression of the polarization curve in the form $V = E^0 - b\cdot\log i - r\cdot i - m\cdot\exp(n\cdot i)$ is reported: the third term has an expression causing an overpotential at open circuit conditions. The parameter m, expressed in V, seems to determine an effect similar to the one caused by the internal current density i_n (in the paper it is specified that the physical meaning of the parameters m and n is not well understood). In the paper, the parameter m is associated to a value in the order of the mV, thus maybe too low to express the reduction of the open circuit voltage due to the internal current density (in the order of 0.15 V).

The dependence of the internal current density from operation variables such as the cell temperature is not discussed in any paper. A functional relation seems to exists: an increase of the operation temperature determines an improvement of the activation of the electrochemical reactions, and thus it could be expected an increase of the internal current density value.

2.4. Limiting current density

The limiting current density is a parameter linked to the concentration overpotential at the electrodes, which is significant just at high load values. In the literature, this parameter is not particularly discussed. In ref. [2], a typical value for a PEM is reported: $i_l = 0.9\ \mathrm{A\,cm^{-2}}$. In the electrochemical literature [6], an analytical expression is described, where the limiting current is function of the diffusion coefficient of the reactant in the electrode, of the electrode thickness and of the reactant concentration above the diffusion in the electrode. Pisani et al. [18] fitted the experimental data of [17] and in case of Nafion 115 fed by H_2/air, operating at atmospheric pressure, at 70 °C the limiting current density is evaluated as $i_l = 0.810\ \mathrm{A\,cm^{-2}}$.

3. The analytical expression adopted for the PEMFC polarization curve

The polarization curve of a single PEM fuel cell can be described by the analytical expression (1):

$$V_c = E - \eta_{act} - \eta_{ohm} - \eta_{conc} \tag{5}$$

where E is the open circuit voltage, η_{act} the activation overpotential in the two electrodes, η_{ohm} the ohmic overpotential (ionic and electronic) and η_{conc} is the concentration overpotential in the two electrodes.

The four terms on the right side of (5) are discussed below.

3.1. Open circuit voltage

The open circuit voltage is usually expressed by Eq. (6) [1,8]:

$$E = \frac{-\Delta\bar{g}(T)}{2\cdot F} + \frac{R\cdot T}{2\cdot F}\cdot\ln\frac{a_{H_2}\cdot a_{O_2}^{0.5}}{a_{H_2O}} \tag{6}$$

If the reactants and the product are assumed as having ideal gas behavior (valid approximation because of the low operating temperatures and pressures [22]), the activity reduces to the ratio of partial pressures [1,8], and the expression (6) is modified in (7):

$$E = \frac{-\Delta\bar{g}(T)}{2\cdot F} + \frac{R\cdot T}{2\cdot F}\cdot\ln\frac{p_{H_2}\cdot p_{O_2}^{0.5}}{p_{H_2O}} \tag{7}$$

where the operation parameters are the temperature and the partial pressures of the reactants and the product in the interface catalyst layer–membrane. The procedure adopted to evaluate the partial pressures in (7) is reported in Appendix A.

3.2. Activation overpotential

The analytical relation between the overpotential and the current density on an electrode surface is expressed by the Butler–Volmer Eq. (8) [1,8]:

$$i = i_{0,el}\cdot\left[\exp\left(\frac{\alpha_a^{el}\cdot F}{R\cdot T}\cdot\eta\right) - \exp\left(-\frac{\alpha_c^{el}\cdot F}{R\cdot T}\cdot\eta\right)\right] \tag{8}$$

If written in explicit form with the electrode overpotential, assuming that the transfer coefficients on an electrode are equal [1,23], the expression (8) becomes:

$$\eta_{act,el} = \frac{R\cdot T}{\alpha^{el}\cdot F}\cdot\sinh^{-1}\left(\frac{i}{2\cdot i_{0,el}}\right) \tag{9}$$

The total activation overpotential in the cell is the sum of the anode and the cathode contributions:

$$\eta_{act} = \eta_{act,c} + \eta_{act,a} = \frac{R\cdot T}{\alpha^{c}\cdot F}\cdot\sinh^{-1}\left(\frac{i}{2\cdot i_{0,c}}\right) + \frac{R\cdot T}{\alpha^{a}\cdot F}\cdot\sinh^{-1}\left(\frac{i}{2\cdot i_{0,a}}\right) \tag{10}$$

The highest activation overpotential is at the cathode, due to the lower value of the exchange current density $i_{0,c}$ [1,6]. The anode and cathode exchange currents are functions of many variables: materials and porosity of the electrode; concentration, distribution and dimension of catalyst particles; operating temperature. The variable which can be modified during operation is the temperature: a temperature increase has a positive effect on the semi-reaction activation on the electrode surface, increasing therefore the exchange current density and reducing the activation overpotential [1,8].

3.3. Ohmic overpotential

The ohmic overpotential has two contributions, linked to the electronic and ionic resistance [1]:

$$\eta_{ohm} = r\cdot i = r^{el}\cdot i + r^{ion}\cdot i \tag{11}$$

The ionic resistance can be expressed as a function of the ionic conductivity and the thickness of the electrolyte membrane:

$$r^{ion} = \frac{t_m}{\sigma} \tag{12}$$

The ionic conductivity is a function of many variables: cell temperature, degree of humidification of the membrane (function of cell temperature, current density, reactants temperature and humidification). A semi-empirical expression has been proposed by Amphlett et al. [14], already reported as Eq. (4). Expression (4) is general, linking the ionic resistance to the temperature, the current density, the membrane thickness and the water content of the membrane λ.

The parameter λ has been introduced by Springer et al. [9], and express the number of water molecules associated to a sulfonic group SO_3^- in the membrane. The degree of humidification of the membrane is linked to the water produced by the cathode semi-reaction (and therefore to the current load), to the inlet water mixed with the reactants (that is, to the degree of humidification of the reactant gases), and to the mass transport phenomena occurring in the membrane [9,15,24–27].

Other models are reported in literature to describe the cell resistance [6,14].

3.4. Concentration overpotential

The concentration overpotential on a electrode can be expressed as [1,8,10,28]:

$$\eta_{\text{conc,el}} = \frac{R \cdot T}{n \cdot F} \cdot \ln\left(1 - \frac{i \cdot \delta}{n \cdot F \cdot D \cdot c_\infty}\right) \tag{13}$$

often expressed introducing the concept of limiting current density:

$$\eta_{\text{conc,el}} = \frac{R \cdot T}{n \cdot F} \cdot \ln\left(1 - \frac{i}{i_{\text{l,el}}}\right) \tag{14}$$

The total concentration overpotential of the cell is the sum of the anode and cathode contributions:

$$\eta_{\text{conc}} = \eta_{\text{conc,c}} + \eta_{\text{conc,a}} = \frac{R \cdot T}{4 \cdot F} \cdot \ln\left(1 - \frac{i}{i_{\text{l,c}}}\right) + \frac{R \cdot T}{2 \cdot F} \cdot \ln\left(1 - \frac{i}{i_{\text{l,a}}}\right) \tag{15}$$

3.5. Internal current

Even at open circuit, the experimental observation shows that the reversible voltage (7) is not reached by the cell. At open circuit, the anodic semi-reaction of hydrogen is at equilibrium, but it could happen that a very limited fraction of the hydrogen molecules oxidize producing H^+ ions and electrons; both diffuse through the membrane (there is not an external load connected) to the cathode side, generating a current. At the same time, there is the possibility that a very limited part of the hydrogen molecules does not participate to the anodic semi-reaction, and diffuse to the cathode in form of molecules (fuel crossover). The two phenomena are modeled as a current flow inside the membrane, introducing the concept of internal current i_n. The internal current could occur also at open circuit conditions, and therefore it could explain the voltage reduction compared to the reversible voltage. Therefore, every value of the current density in Eqs. (10), (11) and (15) is increased by the internal current term i_n [4].

3.6. Analytical expression of the PEMFC polarization curve

The complete analytical expression of the PEMFC polarization curve is:

$$V = \frac{-\Delta\bar{g}(T)}{2 \cdot F} + \frac{R \cdot T}{2 \cdot F} \cdot \ln\frac{p_{H_2} \cdot p_{O_2}^{0.5}}{p_{H_2O}} - \frac{R \cdot T}{\alpha^c \cdot F} \cdot \sinh^{-1}\left(\frac{i + i_n}{2 \cdot i_{0,c}}\right) - \frac{R \cdot T}{\alpha^a \cdot F} \cdot \sinh^{-1}\left(\frac{i + i_n}{2 \cdot i_{0,a}}\right) - r(i + i_n) + \frac{R \cdot T}{4 \cdot F} \cdot \ln\left(1 - \frac{i + i_n}{i_{\text{l,c}}}\right) + \frac{R \cdot T}{2 \cdot F} \cdot \ln\left(1 - \frac{i + i_n}{i_{\text{l,a}}}\right) \tag{16}$$

The expression (16) will be used to fit the experimental polarization curves described in the following.

4. Parameters estimation of the polarization curve

In the analytical expression of the PEMFC polarization curve, Eq. (16), the independent variables are the current density, the temperature and the pressure, while the dependent variable is the voltage. Moreover there are a few constants, that usually are called parameters, and some of these are often unknown. When an experiment is done to obtain the polarization curve, the voltage (dependent variable) is measured directly, but the parameters are not.

The estimation of some of these parameters is an aim of this work. The problem is to obtain the good estimation of these parameters using a discrete number of experimental results, but often not all the parameters can be independently estimate. It is useful to rewrite Eq. (16) in the form:

$$V = f(i, T, p, \alpha^a, \alpha^c, i_{0,a}, i_{0,c}, i_{\text{l,a}}, i_{\text{l,c}}, r, i_n) \tag{17}$$

In Eq. (17), eight parameters are pointed out. For some of these parameters further consideration have been done.

Concerning the transfer coefficient on electrode, it can be defined as [8]:

$$\alpha^a = (1 - \beta) \cdot n_{\text{el}}$$
$$\alpha^c = \beta \cdot n_{\text{el}} \tag{18}$$

where n_{el} is the number of electrons in the rate determining step of the reaction (4 for the anode and 1 for the cathode) and β is a symmetry factor whose value is very near to 0.5 [1,23]; therefore, for the transfer coefficients the values $\alpha^a = 2$ and $\alpha^c = 0.5$ have been assumed.

Concerning the limiting current densities, their values are estimated to be very high (ca. 43 A cm^{-2} for anode and 9 A cm^{-2} for cathode), but in the cell analyzed in this paper the maximum current density imposed is 0.25 A cm^{-2}, because the adopted

MEA (ElectroChem Inc.) showed a sudden voltage drop due to the low ionic conductivity of the membrane. So, we conclude that the effect of the concentration losses is negligible and in our analysis the parameters $i_{l,a}$ and $i_{l,c}$ are not meaningful.

Concerning the area specific resistance r, it could be divided in two components

$$r = r^{el} + r^{ion} \tag{19}$$

where r^{el} is the electronic component and r^{ion} is the ionic. The r^{el} is function of the temperature, while for r^{ion} Amphlett et al. [14] proposed the general law [14,29] already reported in Eq. (4). Fixing λ and t_m, Eq. (4) could be approximated as:

$$r^{ion} \cong C_0(T) + C_2 \cdot i \tag{20}$$

therefore

$$r = r^{el}(T) + C_0(T) + C_2 \cdot i = C_1(T) + C_2 \cdot i \tag{21}$$

Summarizing, Eq. (17) can be now rewritten in the form:

$$V = f(i, i_{0,a}, i_{0,c}, C_1, C_2, i_n) \tag{22}$$

with five parameters unknown.

To verify which parameters can be simultaneously estimated it is useful to analyze the sensitivity coefficients: the ith sensitivity coefficient of a parameter is the first derivate of the function (22) with respect to the ith parameter, multiplied by the ith parameter itself [3]:

$$X_i = \frac{\partial V}{\partial \beta_i}\beta_i \tag{23}$$

When these coefficients, over the range of the observation, are not linearly dependent all parameters can be estimated simultaneously.

To verify if the linear dependence occurs, these coefficients were plotted (Fig. 1): there is a linear dependence between C_1 and C_2 and between C_1 (or C_2) and $i_{0,a}$. Therefore, we decided to estimate the parameter $i_{0,c}$, C_1 and i_n. For the analyzed temperature range, the values of C_2, evaluated through Eq. (4), are shown in Table 1, where from Weber and Newman [15] a value of $\lambda = 14$ has been assumed, valid for a membrane in contact with saturated water, and for the used membrane the thickness was 127 μm.

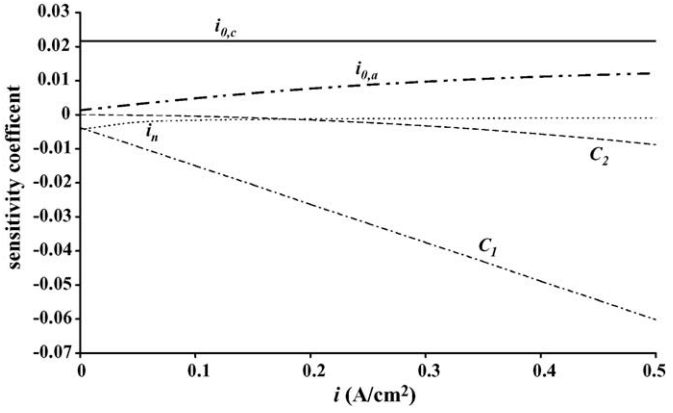

Fig. 1. Sensitivity coefficient vs. current density.

Table 1
Values of the parameter C_2 ($\lambda = 14$, membrane thickness 127 μm in contact with saturated water) in the temperature range 50–80 °C

T (°C)	C_2 ($\Omega\,cm^4\,A^{-1}$)
50	0.0416
55	0.0393
60	0.0372
65	0.0353
70	0.0335
75	0.0318
80	0.0303

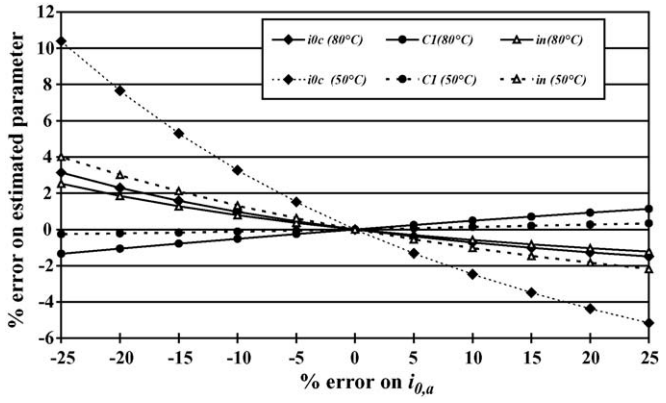

Fig. 2. Relative error on estimated parameters due to an imposed error on $i_{0,a}$.

The exchange current density at the anode $i_{0,a}$ was assumed from literature [4] equal to 0.2 A cm^{-2}. To verify the effect on the parameter estimation of a deviation from this value, an analysis using experimental simulations was done. That is, first some polarization curves were simulated using different value of $i_{0,a}$, then the other parameters were estimated imposing always the reference value of $i_{0,a}$. An analysis imposing a known error on $i_{0,a}$ (±25%) and considering the two extreme temperatures (50 °C and 80 °C) was done. The results of this analysis are shown in Fig. 2: the greater influence was for the parameter $i_{0,c}$ at low temperature, in fact the maximum deviation was 10.4%. At high temperature the maximum effect was less important (3.1%). Also the parameter i_n was influenced from an $i_{0,a}$ error especially at lower temperature (4.0%, compared to 2.5% at higher temperature). On parameter C_1 there was a lower influence when the temperature was high (1.3%) while if low temperature was analyzed the maximum error was very little (0.3%).

5. Experimental

The fuel cell employed for the experiments is an ElectroChem Inc. single cell (EFC25-01SP). This cell employs a Nafion 115 membrane (127 μm thickness), with an active area of 25 cm^2. The electrodes are identical and use Toray^{TM} ca. 0.20 mm thick carbon paper for the backing; the catalyst layer is on the order of ca. 0.05 mm thick so the total electrode thickness is 0.25 ± 0.02 mm. The catalyst layer is made of carbon supported platinum, loading 1 mg cm^{-2} 20 wt.% Pt/C. The membrane electrode assembly (MEA) was first sandwiched between

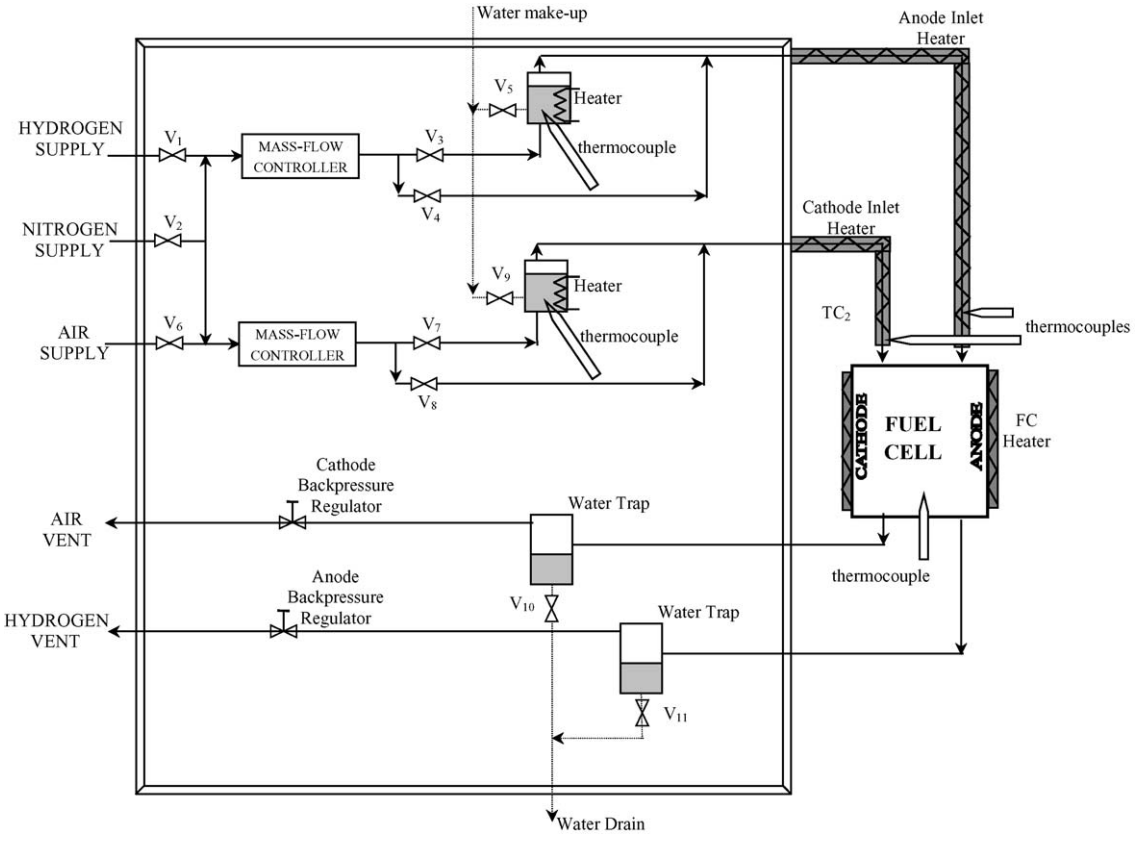

Fig. 3. Schematic drawing of the gas flow apparatus.

two gaskets and then between two graphite current collector plates.

The analyzed fuel cell has been tested with a station made by ElectroChem Inc. (named *Power Station CompuCell*); with this test station three different fluids was managed: the oxidant gas (in this study air), the fuel (hydrogen) and an inert gas for purging purposes (nitrogen). The gas flow rates are controlled with mass-flow controllers. The Gas Management Unit (GMU) can supply humidified or dry gas to the fuel cell. The humidity is imposed by sparging the gases through two gurgle tanks filled with distilled water. The tanks are heated and kept at the chosen temperatures by controllers. The temperature sensors are K-type thermocouples. The scheme of the experimental apparatus is shown in Fig. 3.

A set of experimental tests has been scheduled to analyze the effects of the temperature on cell performance and especially on the behavior of some characteristic parameters (exchange and internal current densities; membrane resistance). To outline the temperature effect, the tests have been carried out imposing the cell temperature in the range $T = 50$–$80\,^{\circ}\mathrm{C}$ (maximum design temperature of the experimental setup), with a temperature step of $5\,^{\circ}\mathrm{C}$ (with 7 runs for every session); the number of sessions has been 5, and therefore the total number of runs has been 35. The same temperature has been adopted for both the inlet streams, and moreover they were in saturation conditions, therefore $T = T_a^S = T_c^S$. The tests have been performed at ambient pressure (reactant backpressures fixed to zero).

The available test facility does not allows an automatic modification of the reactant mass flows according to the load, and therefore operates with a constant mass flow during the runs. The maximum value of the cell current density has been fixed at $0.25\,\mathrm{A\,cm^{-2}}$ (7.5 A), but the volume flow values were fixed in order to reach a higher current load ($0.8\,\mathrm{A\,cm^{-2}}$): $141\,\mathrm{ml\,min^{-1}}$ of hydrogen (excess $\lambda_H = 1.2$) and $726\,\mathrm{ml\,min^{-1}}$ of air (excess $\lambda_{air} = 2$). As these volume flows are fixed, a further excess of hydrogen and air at low current densities occurs.

Some preliminary experiments were carried out to choose the load profile that was then adopted in the tests. As observed above, the maximum current density was fixed at $0.25\,\mathrm{A\,cm^{-2}}$. The current density therefore varies between $0\,\mathrm{A\,cm^{-2}}$ and $0.25\,\mathrm{A\,cm^{-2}}$ with steps of $0.025\,\mathrm{A\,cm^{-2}}$. Every current density plateau is kept for 30 s, and the ramp between the plateau also lasts 30 s. Therefore, the total test length was ca. 11 min. The sampling rate for data logging was 1 s. The considered voltage was the average value, and the estimated maximum voltage uncertainty is less than 3%.

6. Results and comments

6.1. Regression analysis

Fig. 4 shows how the model can rebuild the polarization curve of the cell when the unknown parameters are estimated at a fixed temperature. In the figure the regression curves obtained at different values of the temperature range (lower bound:

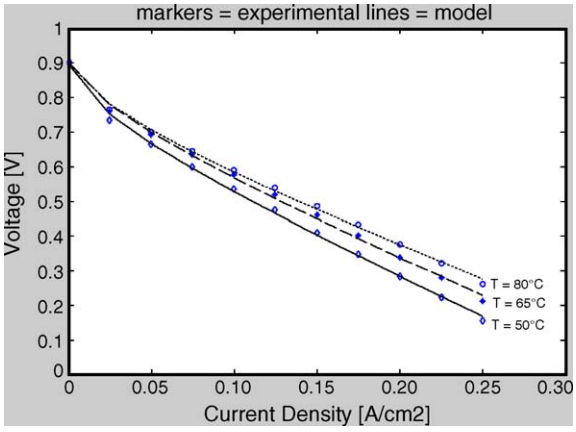

Fig. 4. Regression curves obtained at different values of the temperature range—50 °C: rhombus experimental, solid line model; 65 °C: asterisks experimental, dashed line model; 80 °C: circles experimental, dotted line model. Maximum voltage uncertainty less than 3%.

50 °C; intermediate value: 65 °C; upper bound: 80 °C) are shown.

As it was expected, the activation of the reactions is facilitated at higher temperatures (lower activation overpotential), and the cell resistance is lower at higher temperatures (lower slope of the curve). From the graph it is possible to see that the analytic curves rebuild the experimental markers very satisfactorily. We only notice a bigger distance between the markers and the curves at 0.025 A cm^{-2}: we think this fact is due to the estimation of the cathode exchange current density, which is the parameter most sensitive to errors and the most important parameter for the part of the curve where the imprecision has been noticed.

Concerning the performance of the adopted MEA (ElectroChem Inc.), it is evident that the cell overpotentials are very high: at a low value of current density (e.g. 0.2 A cm^{-2}) the cell voltage is already dropped at values around 0.4 V. As shown in Fig. 4, the sudden voltage drop is mainly due to a low ionic conductivity of the membrane, and this effect is confirmed by the high values obtained by the parameter C_1 of Eqs. (20) and (21) modeling the cell resistance, which are discussed below. Nevertheless, the analysis of the performances of the MEA do not represent the aim of the paper, which concentrates on the discussion of the MEA model and of the regression procedures applied to experimental data to estimate some important cell parameters.

6.2. Dependence of $i_{0,c}$ with temperature

In Fig. 5, the estimated values and the error bars of the parameter $i_{0,c}$ versus the operating temperatures are shown.

Concerning the obtained values, they are coherent with other values indicated in literature [4–13]. In particular, the trend of the parameter with temperature seems very similar to the trend reported by Parthasarathy et al. [13], and this could confirm the validity of the adopted model and especially of the parameter estimation procedure. From the graph, it is possible to observe a qualitative behavior of the parameter: it increases with temperature, and the slope of the function is close to a constant value in

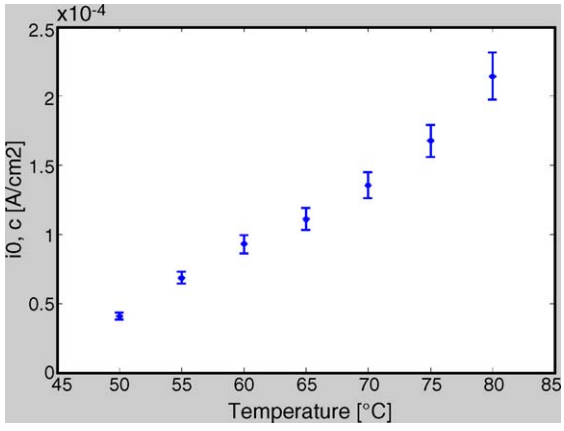

Fig. 5. Values of the parameter $i_{0,c}$ vs. cell operating temperature.

the range 50–75 °C (nearly a linear shape); then a slope increment occurs at greater temperatures. The absolute values of the parameter are lower than the ones obtained by Parthasarathy et al. [13], and this is linked to the observed low quality of the MEA; nevertheless, the values are of the same order of magnitude (10^{-4} A cm^{-2}), marking that the cathode activation overpotential does not represent the main cause of the low performance of the MEA. The estimated uncertainty of this parameter is ±10%.

6.3. Dependence of r (C_1) with temperature

In Fig. 6, the estimated values and the error bars of the parameter C_1 versus the operating temperatures are shown.

The trend of the parameter with temperature is the expected one, typical of the electrolytes (ionic conductors): the qualitative behavior shows a quite linear decrease in the range of temperatures from 50 °C to 80 °C. The absolute values of the parameter are consistently higher than the ones reported in literature related to other MEAs: the obtained value is in the range 1.6–1.9 Ω cm^2 (estimated uncertainty is less than ±1%), while typical values are in the order of 0.3 Ω cm^2 [5,6,9,14,16]. As discussed above in case of $i_{0,c}$, this is linked to the evident low quality of the tested MEA: in particular, these values of cell resistance, and the related high values of ohmic overpotentials, seem to represent the main cause of the low performance of the MEA.

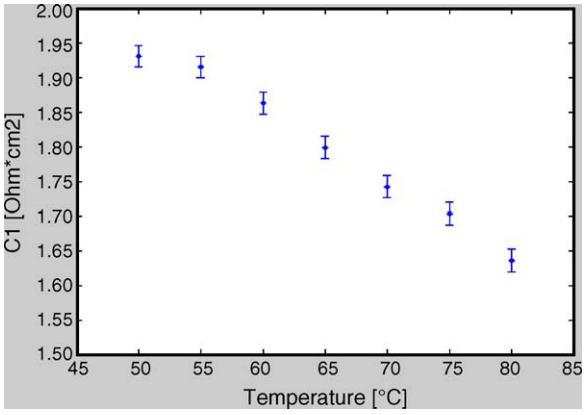

Fig. 6. Values of the parameter C_1 vs. cell operating temperature.

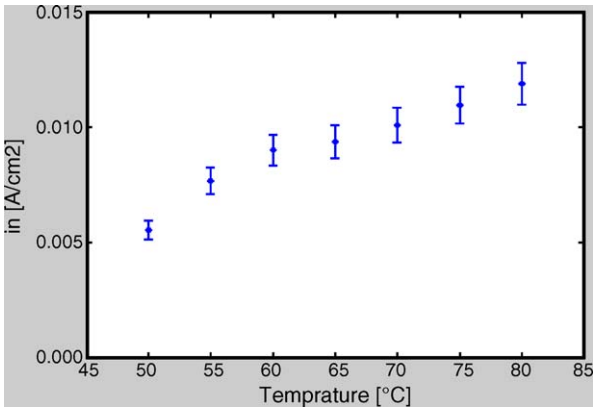

Fig. 7. Values of the parameter i_n vs. cell operating temperature.

6.4. Dependence of i_n with temperature

In Fig. 7, the estimated values and the error bars of the parameter i_n versus the operating temperatures are shown.

As stated above, in literature we have not found descriptions of a possible trend of this parameter with temperature. The trend observed with our data shows an increase of the parameter with temperature in the range from 50 °C to 80 °C. The absolute values of the parameter are higher than the only case reported in literature [4]: the obtained value is in the range 6–12 mA cm^{-2} (estimated uncertainty is ca. ±7%), compared with the value indicated by Larminie and Dicks which is in the order of 2 mA cm^{-2}. Apparently, these values seem to represent another cause of the low performance of the adopted MEA, because a high value of in means an increase of the fuel crossover. At the same time, the trend increasing with temperature seems to suggest that the crossover phenomena occurs with higher probability at increased temperatures. The last sentences have to be analyzed in more detail with other experimental sessions.

7. Application of the regression model to the experimental data of other authors and discussion

To give some evidence of the validity of the regression model and procedure, they have been extended to other sets of experimental data, besides the experimental sessions produced in our laboratory. Experimental data in form of polarization curves of single cells are largely available in literature. Unfortunately, not many papers report also the results of the fitting procedure in terms of the values of the parameters of the polarization curve with their uncertainty; these values are necessary in order to check the regression model and procedure. We have considered in particular two papers [16,17]. Both the papers report experimental data in form of polarization curves, and especially report the estimated values of one of the parameters considered in our paper: the cell resistance r (actually, our model has separated the cell resistance in an expression with two parameters, Eq. (21), but from the values of C_1 and C_2 we can obtain r).

As shown in Table 2, the values of r found with our regression model are in good agreement with the values of the parameter reported by Kim et al. The values estimated by our regression model are slightly lower than the values reported by Kim et al.: therefore, we assign a lower value to the ohmic overpotential. A possible explanation can be linked to the role and values of the cathode exchange current density parameter $i_{0,c}$. We have tried to estimate the values of the parameter from the data available by the paper. The model indicates as $E_0 = E_r + b \cdot \log i_0$, with E_0 is the fitted parameter, E_r the reversible potential for the cell, and i_0 and b are the Tafel parameters for oxygen reduction. The values of E_0 and b are reported by Kim et al.; the value of E_r can be read in Figs. 4 and 5 of [16] (with some approximation); finally, the value of i_0 can be estimated in the order of 5–6 × 10^{-1} A cm^{-2}. These values are higher than other values reported in literature (in the order of 1–2 × 10^{-4} A cm^{-2}) and even than the values estimated by our regression model (in the order of 3–4 × 10^{-4} A cm^{-2}). This means that, according to the estimated values, the cathode activation overpotential are very low in the regression model used by Kim et al. This causes the fact that their regression model has to assign a greater weight to the ohmic overpotential, explaining the higher values of the parameter r compared by the values found by our regression model. Maybe the regression model used by Kim et al. underestimates the weight of the cathode activation overpotential, which is not negligible compared to the ohmic overpotential (see, for example [31], Fig. 4, p. 2483).

Concerning the behavior of r versus T the slope is 5.7 × 10^{-3} Ω cm^2 K^{-1} for our experimental results and a slope of 6.2 × 10^{-3} Ω cm^2 K^{-1} for Kim et al. experimental results. These results are in good agreement.

Concerning the paper of Squadrito et al. [17], the discussion is similar. As shown in Table 2, the values of r found with our regression model are lower than the values reported by Squadrito et al. But, as reported in Squadrito et al. (p. 1454), the expected values were in the order of 0.12–0.14 Ω cm^2, in accordance with the value estimated by our regression model applied to the data provided by the authors. In our opinion, even in this case a possible explanation can be linked to the role and values of the cathode exchange current density parameter.

Table 2
Comparison between the values of the cell resistance evaluated with our regression model and the values reported by Kim et al. [16] and Squadrito et al. [17]

Cell temperature (°C)	Data from Kim et al. [16]		Data from Squadrito et al. [17]	
	Eq. (16), our paper (Ω cm^2)	Eq. (5) [16] (Ω cm^2)	Eq. (16), our paper (Ω cm^2)	Eq. (5) [17] (Ω cm^2)
50	0.323	0.363	–	–
70	0.208	0.238	0.135	0.240

Membrane: Nafion 115; reactant: H_2/air; pressure: 1 atm.

8. Conclusions

The paper describes a methodology for the estimation of some parameters of the model of the polarization curve of the cell, and analyzes and discusses the behavior of the parameters versus a fundamental independent variable (the cell operating temperature). The results can be summarized as follows:

- from the parameters analysis it has been verified that only three parameters of the cell polarization curve model can be simultaneously estimated: $i_{0,c}$, C_1 and i_n; the low sensibility of the model due to the effects of the other parameters has been demonstrated using experimental simulations;
- the analytical model of the polarization curve rebuilds the experimental results very satisfactorily; the regression is less accurate at low current densities, probably due to the estimation of the cathode exchange current density which is the parameter most sensitive to errors;
- the qualitative behavior of the parameter $i_{0,c}$ shows a quite linear increase in the range of temperatures from 50 °C to 80 °C, with values in coherence with the literature reports (10^{-4} A cm^{-2});
- the trend of the parameter C_1 (linked to the cell resistance) is typical of the electrolytes, with a quite linear decrease with temperature;
- the qualitative behavior of the parameter i_n shows an important increase in the range of temperatures from 50 °C to 80 °C; the increase with temperature seems to suggest that the crossover phenomena occurs with higher probability at increased temperatures;
- due to the limited numbers of experimental points, and especially to the fact that the experiments have been done using just one MEA, it is not possible to propose general analytic correlations linking the parameters and the operating temperature, but the potentiality of the method of analysis and the easiness of the experiments allow to apply it for a wide typologies of MEAs; in fact we have checked the regression model with data of cell resistance provided by other authors with good agreement of the results.

Acknowledgments

The authors wish to thank the Hydrogen System Laboratory (HySyLab) of the Environment Park of Torino for the support in the experimental session of the present work.

Appendix A. Procedure adopted to evaluate the partial pressures in Eq. (7)

The partial pressures at the interface are evaluated through laws of diffusion in porous media [5,29–33]. Considering the flow in the inlet ducts of the bipolar plate, a mass fraction diffuses through the electrode diffusion layer. The mass transport has been considered perpendicular to the diffusion layer surface. To evaluate the molar fraction y of each component of the mixed flow after the diffusion layer (that is, in correspondence of the catalyst layer) the Stefan–Maxwell equation has been used [34]:

$$\nabla y_i = \sum_{j=1}^{n} \frac{R \cdot T}{p \cdot D_{ij}} \cdot (y_i \cdot N_j - y_j \cdot N_i) \tag{A1}$$

where N is the molar flux of a component per unit surface. The binary diffusion coefficient D_{ij} have been evaluated through expression (A2):

$$p \cdot D_{A,B} = a \cdot \left(\frac{T}{\sqrt{T_{cA} \cdot T_{cB}}} \right)^{b} \cdot (p_{cA} \cdot p_{cB})^{1/3} \cdot (T_{cA} \cdot T_{cB})^{5/12} \cdot \left(\frac{1}{\bar{M}_A} + \frac{1}{\bar{M}_B} \right)^{1/2} \tag{A2}$$

where the coefficients a and b depend on the mixture and are reported in [34].

The effective diffusivity in the porous diffusion layer has to be evaluated from the binary diffusion coefficient. There are different models proposed to evaluate the effect of porosity ε of the transport medium [5]. We have considered the correlation suggested by [35], valid for random fibrous porous media representing the diffusion layer of the cell electrode:

$$D_{eff} = D_{A,B} \cdot \varepsilon \cdot \left(\frac{\varepsilon - \varepsilon_p}{1 - \varepsilon_p} \right)^{\gamma} \tag{A3}$$

Concerning the porosity, in absence of specific data for our cell, we have considered a value widely used in literature: $\varepsilon = 0.3$ [6]. The parameter ε_p is a percolation threshold: for porous media composed of two-dimensional, long and overlapping random fibber layers, it has been found as 0.11 [5]. The term γ is an empirical constant, found as 0.785 in case of cross-plane diffusion [5].

The molar flux per surface area N represents the net number of moles of a chemical species transported through the diffusion layer to the membrane interface of active surface S for unit time. The number of moles participating to the reaction for unit time and surface is evaluated with the Faraday law—concerning hydrogen and oxygen we have:

$$N_{H_2} = \frac{I}{2 \cdot F \cdot S} = \frac{i}{2 \cdot F}, \qquad N_{O_2} = \frac{I}{4 \cdot F \cdot S} = \frac{i}{4 \cdot F} \tag{A4}$$

Nitrogen is inert, and thus its net flux through the diffusion layer is $N_{N_2} = 0$. Concerning the water molar flux, we have to consider both the inlet water (with humidified reactant flows) and the transport mechanisms inside the membrane. The electro-osmotic drag of water from anode to cathode is described through [24,36]:

$$N_{H_2O,eo} = n_d \cdot \frac{i}{F} \tag{A5}$$

where n_d is the electro-osmotic drag coefficient. In literature, different values of n_d can be found, directly linked to the degree of humidification of the membrane [9,15,36]; using the experimental data described in [24], we have estimated the value $n_d = 0.27\ \mathrm{mol}_{H_2O}\ \mathrm{mol}_{H^+}^{-1}$. The other transport mechanism is the

bask diffusion from cathode to anode, linked to the concentration gradient at the two sides of the membrane (with higher value at the cathode). The molar flux of water due to back diffusion is expressed by [9,34,36]:

$$N_{H_2O,bd} = D_w \cdot \frac{c_{H_2O,c} - c_{H_2O,a}}{t_m} \quad (A6)$$

The water diffusion coefficient D_w is evaluated through expressions found in [9] as $D_w = 1.28 \times 10^{-10}\ m^2\ s^{-1}$.

The molar flux of water to the anode reaction site coming from the channels (from the humidified reactant flow) is $N_{H_2O,a}$; a fraction migrates to the cathode via electro-osmosis drag, while another molar flux diffuses to the anode via back diffusion from the cathode reaction site; the net water molar flux through the membrane (positive if directed to cathode) is therefore:

$$N_{H_2O,net} = N_{H_2O,eo} - N_{H_2O,bd} \quad (A7)$$

The water molar flux which returns from the anode reaction site to the anode channels is thus $N_{H_2O,a} - N_{H_2O,net}$. So, the net water molar flux transported through the anode diffusion layer is evaluated as:

$$N_{H_2O,a,net} = N_{H_2O,a} - (N_{H_2O,a} - N_{H_2O,net}) = N_{H_2O,net} \quad (A8)$$

At the cathode, $N_{H_2O,c}$ is the molar flux of water to the cathode reaction site from the channels (from the humidified reactant flow); $N_{H_2O,net}$ is the molar flux coming from the membrane; moreover, $N_{H_2O,prod}$ is the molar flux of produced water. Therefore, the net water molar flux transported through the cathode diffusion layer is:

$$N_{H_2O,c,net} - (N_{H_2O,c} + N_{H_2O,prod} - N_{H_2O,net}) = -(N_{H_2O,net} - N_{H_2O,prod}) \quad (A9)$$

where the negative sign stands for a flux from the catalyst layer to the distribution channels. There are all the details to solve the differential equation (A2).

References

[1] E. Barendrecht, Electrochemistry of fuel cells, in: L.J.M.J. Blomen, M.N. Mugerwa (Eds.), Fuel Cell Systems, Plenum Press, New York, 1993.

[2] J.H. Lee, T.R. Lalk, A.J. Appleby, Modeling electrochemical performance in large scale proton exchange membrane fuel cell stacks, J. Power Sources 70 (1998) 258–268.

[3] J.V. Beck, K.J. Arnold, Parameter Estimation in Engineering and Science, John Wiley & Sons, New York, 1977.

[4] J. Larminie, A. Dicks, Fuel Cell Systems Explained, John Wiley & Sons Ltd., Chichester, GB, 2000.

[5] J.H. Nam, M. Kaviany, Effective diffusivity and water-saturation distribution in single- and two-layer PEMFC diffusion medium, Int. J. Heat Mass Transfer 46 (2003) 4595–4611.

[6] J.C. Amphlett, R.M. Baumert, R.F. Mann, B.A. Peppley, P.R. Roberge, Performance modelling of the Ballard Mark IV solid polymer electrolyte fuel cell, J. Electrochem. Soc. 142 (1995) 1–15.

[7] C. Berger, Handbook of Fuel Cell Technology, Prentice Hall, Englewood Cliffs, NJ, 1968.

[8] G. Prentice, Electrochemical Engineering Principles, Prentice Hall International, Houston, USA, 1991.

[9] T.E. Springer, T.A. Zawodzinski, S. Gottsfeld, Polymer electrolyte fuel cell model, J. Electrochem. Soc. 138 (1991) 2334–2341.

[10] L. You, H. Liu, A parametric study of the cathode catalyst layer of PEM fuel cells using a pseudo-homogeneous model, Int. J. Hydrogen Energy 26 (2001) 991–999.

[11] L. You, H. Liu, A two-phase flow and transport model for the cathode of PEM fuel cells, Int. J. Heat Mass Transfer 45 (2002) 2277–2287.

[12] D. Bevers, M. Wohr, K. Yasuda, K. Oguro, Simulation of a polymer electrolyte fuel cell electrode, J. Appl. Electrochem. 27 (1997) 1254–1264.

[13] A. Parthasarathy, S. Supramaniam, A.J. Appleby, C.R. Martin, Temperature dependence of the electrode kinetics reduction at the platinum/Nafion interface—a microelectrode investigation, J. Electrochem. Soc. 139 (1992) 2530–2537.

[14] R.F. Mann, J.C. Amphlett, M.A.I. Hooper, H.M. Jensen, B.A. Peppley, P.R. Roberge, Development and application of a generalised steady-state electrochemical model for a PEM fuel cell, J. Power Sources 86 (2000) 173–180.

[15] A.Z. Weber, J. Newman, Transport in polymer-electrolyte membranes. I. Physical model, J. Electrochem. Soc. 150 (2003) 1008–1015.

[16] J. Kim, S.M. Lee, S. Srinivasan, C.E. Chamberlin, Modeling of proton exchange membrane fuel cell with an empirical equation, J. Electrochem. Soc. 142 (1995) 2670–2674.

[17] G. Squadrito, G. Maggio, E. Passalacqua, F. Lufrano, A. Patti, An empirical equation for polymer electrolyte fuel cell (PEFC) behaviour, J. Appl. Electrochem. 29 (1999) 1449–1455.

[18] L. Pisani, G. Murgia, M. Valentini, B. D'Aguanno, A new semi-empirical approach to performance curves of polymer electrolyte fuel cells, J. Power Sources 108 (2002) 192–203.

[19] V. Ramani, H.R. Kunz, J.M. Fenton, Investigation of Nafion/HPA composite membranes for high temperature/low relative humidity PEMFC operation, J. Membrane Sci. 232 (2004) 31–44.

[20] V. Ramani, H.R. Kunz, J.M. Fenton, Stabilized heteropolyacid/Nafion® composite membranes for elevated temperature/low relative humidity PEFC operation, Electrochim. Acta 50 (2005) 1181–1187.

[21] J.M. Corrêa, F.A. Farret, V.A. Popov, M.G. Simões, Sensitivity analysis of the modeling parameters used in simulation of proton exchange membrane fuel cells, IEEE Trans. Energy Convers. 20 (2005) 211–218.

[22] E.P. Gyftopoulos, G.P. Beretta, Thermodynamics: Foundations and Applications, MacMillan Publishing Company, NY, USA, 1991.

[23] T. Zhou, H. Liu, A general three-dimensional model for proton exchange membrane fuel cells, Int. J. Trans. Phenom. 3 (2001) 177–198.

[24] W.K. Lee, S. Shimpalee, J.W. Van Zee, Verifying predictions of water and current distribution in a serpentine flow field polymer electrolyte membrane fuel cell, J. Electrochem. Soc. 150 (2003) 341–348.

[25] M. Cappadonia, J.W. Erning, S.M. Saberi Niaki, U. Stimming, Conductance of Nafion 117 membranes as a function of temperature and water content, Solid State Ionics 77 (1995) 65–69.

[26] P. Berg, K. Promislow, J. St.-Pierre, J. Stumper, B. Wetton, Water management in PEM fuel cells, J. Electrochem. Soc. 151 (2004) A341–A353.

[27] A. De Zan, Model development and experimental analysis of the water mass transport mechanisms in the membrane of a PEMFC, Master Thesis, DENER Politecnico di Torino, 2004.

[28] L.R. Jordan, A.K. Shukla, T. Behrsing, N.R. Avery, B.C. Muddle, M. Forsyth, Diffusion layer parameters influencing optimal fuel cell performance, J. Power Sources 86 (2000) 250–254.

[29] P. Cochis, Experimental analysis of a PEMFC to estimate its main operation parameters, Master Thesis, DENER Politecnico di Torino, 2004.

[30] M.W. Verbrugge, D.M. Bernardi, Mathematical model of a gas diffusion electrode bonded to a polymer electrolyte, AIChE J. 37 (1991) 1151–1162.

[31] D.M. Bernardi, M.W. Verbrugge, A mathematical model of the solid polymer-electrolyte fuel cell, J. Electrochem. Soc. 139 (1992) 2477–2491.

[32] S.J. Ridge, R.E. White, Y. Tsou, R.N. Beaver, G.A. Eisman, Oxygen reduction in a proton exchange membrane test cell, J. Electrochem. Soc. 136 (1989) 1902–1909.

[33] R.P. Iczkowski, M.B. Cutlip, Voltage losses in fuel cell cathodes, J. Electrochem. Soc. 127 (1980) 1433–1439.
[34] R.B. Bird, W.E. Stewart, E.N. Lightfoot, Transport Phenomena, John Wiley & Sons Inc., London, 1963 (third printing).
[35] M.M. Tomadakis, S.V. Sotirchos, Ordinary and transition regime diffusion in random fiber structures, AIChE J. 39 (1993) 397–412.
[36] S. Shimpalee, S. Dutta, Numerical prediction of temperature distribution in PEM fuel cells, Num. Heat Transf. 38 (Part A) (2000) 111–128.